

Structural Changes in the Prostate of Old Rats with Chronic Alcoholism

Received: 19 February 2023, **Revised:** 21 March 2023, **Accepted:** 25 April 2023

Radjabov Akhtam Boltaevich

Bukhara, Uzbekistan, postal code 200100

Bukhara State Medical Institute named after Abu Ali ibn Sina, Uzbekistan,

Bukhara, A.Navoi str.1 Tel: +998(65) 223-00-50 e-mail: info@bsmi.uz, raxtam@list.ru.

<https://orcid.org/0000-0003-2945-8560>

Keywords:

prostate, chronic drinking, gland morphometry, acinus, and rats

Abstract

Morphological and structural alterations in the prostate of aged rats due to prolonged drinking are discussed in this article. 18-month-old animals show moderate lymphocytic infiltration without tissue damage and lymphoid nodular development along with other modifications such as proliferative changes in the epithelium of the secretory sections, the detection of nodules inside the acini, and congestive, vascular abnormalities. As chronic alcoholism progresses in animals, the glandular parenchyma of the affected organs shrinks, lymphocytic infiltration causes tissue damage, and lymphoid nodules appear. As shown in the experiment, papillary structures develop and expand as a result of involutive changes including flattening of the acinar epithelium, reduction in the size of the acinus, and suppression of secretory activity.

1. Relevance

Heavy drinking is a common problem in today's culture. In one way or another, ethyl alcohol affects practically all organs and tissues due to its absorption into the blood and its chemical features, resulting, depending on its quantity, to the development of alterations of a dystrophic and destructive nature [3, 4, 6, 7, 9, 10, 11, 12, 13].

The morphology of the prostate in old age and under chronic alcohol exposure has not been practically examined comprehensively, thus there is need for improvement in describing the morphometry of all glandular and non-glandular components. As such, there is undeniable academic and practical interest in studying the morphological properties of an organ under situations of prolonged alcohol exposure. If this problem were to be investigated, more information would be made public about how chemical environmental influences harm reproductive organs.

2. The Purpose Of Our Research

The goal of this study was to compare the epithelial-stromal features of the prostate in aged rats to those in rats who had been chronically exposed to alcohol.

3. Materials and Methods

Twenty 1.5-year-old male outbred white rats were used in the investigation. There were 20 participants split evenly between 2 groups: 10 in the control group and 10 in the experiment group.

Animals in the experimental group were injected with a 40.0% ethanol solution to simulate persistent alcoholism [8]. For one month before to the study age, the solution was injected intragastrically using a metal probe once daily at a total dosage of 7 g/kg of body weight. Non-treatment animals had the same amount of 0.9% NaCl solution injected into their gastrointestinal tracts. In accordance with established protocols [5], rats were sacrificed by being instantly beheaded while under the effects of ether.

Prostate tissue samples were formalin-fixed (10% buffered) and paraffin-embedded (the gold standard) for histological analysis. Hematoxylin and eosin were used to analyze histological sections cut from paraffin blocks, and van Gieson staining was used to identify collagen fibers.

The sections were found using a microscope magnified 70 times (7x) to find:

Journal of Coastal Life Medicine

- the number of intralobular stromal vessels and the number of intraorgan vessels were counted; - the shape of the gland lumen was recorded; - the number of terminal sections of the glands in the field of view was recorded; - the volume fraction of acini with and without secretion (in%) was recorded; - the number of acini with desquamated epithelial cells was recorded;

The ocular micrometer was used to measure the diameter of the lumen of the glands, the height of the epithelium, and the inner diameter and wall thickness of intraorganic vessels in the preparations at a magnification of 280 times (7x40). Additionally, collagen fiber thickness and dispersion among the gland's tissues were measured.

Lymphocytic infiltration into glandular tissues was evaluated for presence and degree within the field of view (7x40). The North American Chronic Prostatitis Collaborative Research Network and the International Prostatitis Collaborative Network categorization systems were used to allocate lymphocytes according to disease severity (cell density):

1) Confluent fields of lymphocytic cells without tissue destruction and / or lymphoid nodular / follicular formation are indicative of a moderate degree of lymphocytic infiltration; confluent fields of lymphocytic cells with tissue destruction and / or lymphoid nodular / follicular formation are indicative of a severe degree of lymphocytic infiltration.

The thickness of the stroma layers between the glands was measured using an eyepiece micrometer at a magnification of the objective x40, ocular x7 in the field of vision to evaluate the severity (fibrosis) of the proliferation of connective tissue in the experiment.

The suitable approach [2] (fields of vision, scored out of ten) was used to assess the degree of connective tissue compaction. Forms 2 and 3 are more apparent, with form 2 characterized by stromal septa enlargement up to twice their normal size in four or more fields of view, and form 3 characterized by stromal septa enlargement up to three times their normal size in seven to ten fields of view.

The glandular and stromal element volume fractions (in %) were analyzed. This was accomplished by counting the number of intersections falling on the stromal and glandular (including the lumen of the gland) elements using the morphometric grid [1] (with the number of

intersections 100) with an eyepiece x10 and a lens x10 in each preparation of the prostate in 10 fields of view.

4. Results and Discussion

Secretory end sections and connective tissue stroma, including smooth myocyte and vascular bundles, make up the prostate in rats 1 and a half years old.

Scanning electron microscopy reveals that the acini are irregular and oval in shape. The secretory terminal villus is lined with cuboidal or, less often, highly prismatic epithelium (Fig. 1). The average thickness of an epithelial layer is 8.4042 m, however it may range from 4.2m to 12.6m. It is possible, in certain preparations, to observe areas of cell development in the prostatic urethra and excretory duct epithelium, which are distinguished by their dark color due to the high density of epitheliocytes. Some of the hyperplastic lymph nodes exhibit cystic atrophy (Figure 3). Gland lumens typically vary in size from 252.0 to 504.0 microns in diameter. The range of acini counts per visual field is 18-34, with an average of 25.90.9. There are 90-100% acini with a secret, with an average of 95.0 0.5 %, and up to 10% acini without a secret, with an average of 5.0 0.5 %. Half of the time, concretions within the acini are between 5 and 15 m in size, whereas bigger concretions are only seen in pristine specimens. Several areas of the epithelial lining have been broken through, as seen in Fig. 4.

Lymphocytes are identified in confluent diffuse accumulations in the periglandular stroma and at specific sites around the arteries of the stroma (Fig. 2), but there is no evidence of tissue breakdown or lymphoid nodular formation. The median lymphocyte count was 29, while the range was 20-35 lymphocytes per visual field. In the central areas of the gland, the secretory sections are packed tightly together due to the acini's excessive development, leaving almost no stroma between them. As a result, the thickness of the partitions might fluctuate between 4 and 12 microns. The subcapsular zone is dominated by the stroma, and the stromal septa that divide the acini range in thickness from 50.4, on average, to 168.0 m. Visible stromal vessels range in number from 11 to 15, with an average of 13.00.2. In most specimens, blood is present inside the lumens of almost all vessels, most notably venules. Figure 2 shows lymphocyte accumulation and infiltration into vessel walls. Venules typically have an inner diameter between 25.2 and 33.6 microns, with a mean value of 30.70.42 microns. Their thickness varies between 4.2 and 8.4 microns, with an average of 7.9 0.21 microns. The average diameter of a capillary is 16.3 0.21 m, with a range of 12.6 m to 16.8

m. The average wall thickness is 6.470.21 microns, with a range of 4.2-8.4 microns. The diameters of arteries' interiors range from 12.6 to 16.8 m, with 15.75 0.21 m serving as an average. Their thickness may vary from

4.21 meters to 8.40 meters. Between 45 to 75% of the total volume of the body is made up of glandular tissue, with an average of 61.3% 1.6%. On average, stromal tissue accounts for 38.7 1.6% of the total tissue volume.

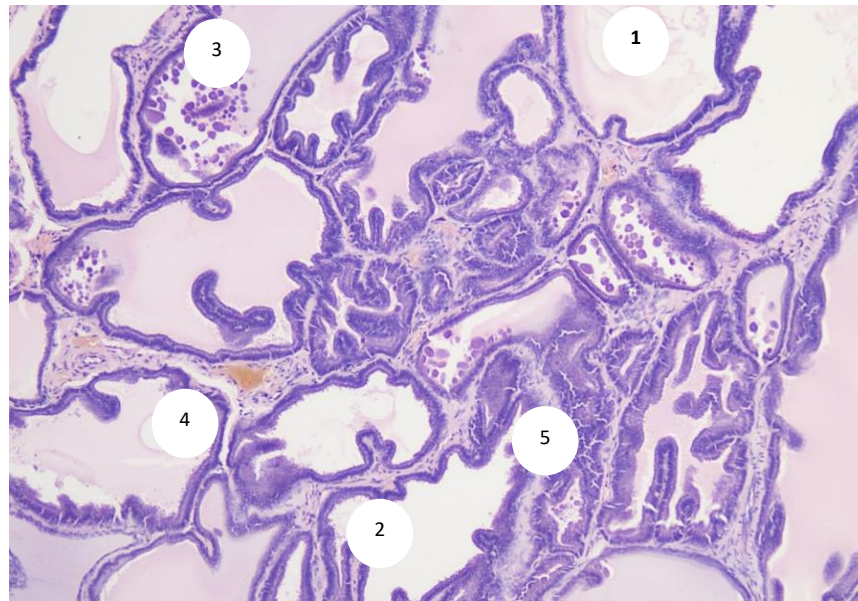


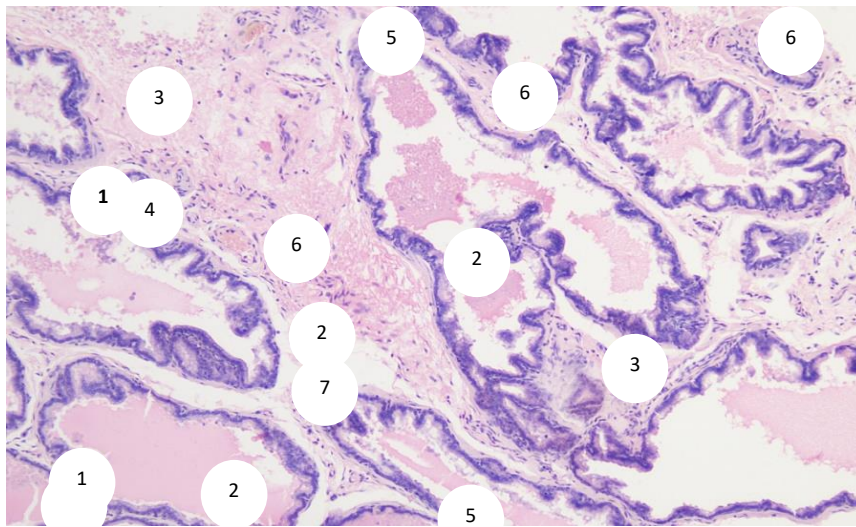
Figure.1. The prostate of a rat that is 18 months old. Hematoxylin and eosin staining. 1) irregularly shaped acini, 2) acini with intraluminal secretion, 3) concretions inside the secretory sections, 4) many stromal capillaries, and 5) widespread lymphocyte accumulations in the stroma. In that case, ten copies of volume 20 is OK.

Most collagen fibers are found beneath the epithelium, forming a small-loop network in the stroma; nevertheless, holes may be seen at certain locations, indicating a breach in the epithelial barrier (Fig. 4). Bundles of collagen fibers may range in thickness from 4.2 to 12.3 m, with 10.5 0.42 m serving as the mean.

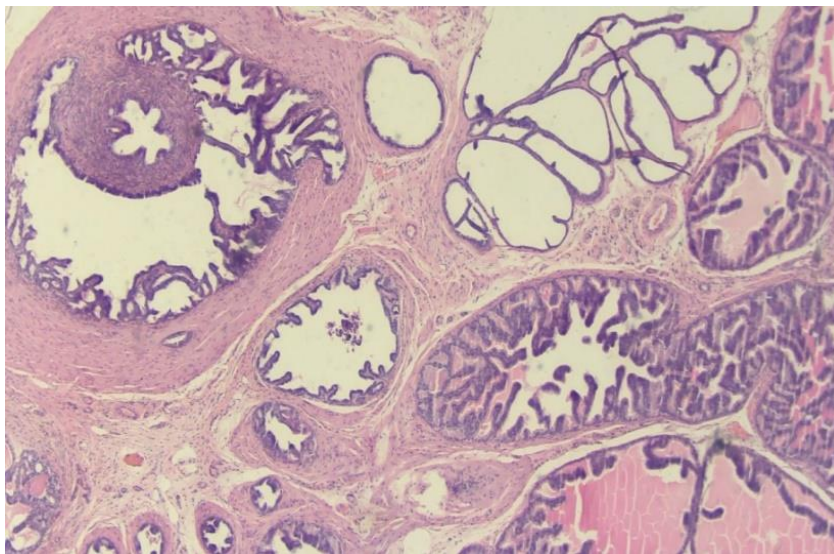
Eighty percent of the acini in the study's experimental group of 18-month-old rats were found to have a folded look with epithelial-stromal outgrowths, to be represented by cuboidal epithelium, and to be characterized in parts by squamous epithelium (Fig. 5). Epithelial lining thickness ranges from 4.2 to 8.4 m, with an average of 5.8 0.21 m.

Epithelial stratification foci are identified, and epithelial layering disruption, cell polymorphism, the presence of large and numerous nucleoli in the nuclei, and the visualization of mitotic cells are also seen (Fig. 6). The acini lumens are convoluted (Fig. 5), and the terminal parts of the glands are mostly irregular and oval in form. The average size of a gland's lumen is 288.58.8 microns, with a range of 210.0-420.0 microns. How many acini are seen in the eye's frame of vision

of lymphocytes around the stromal vessels, 7-cells of connective tissue. OK. 10 x vol. 25



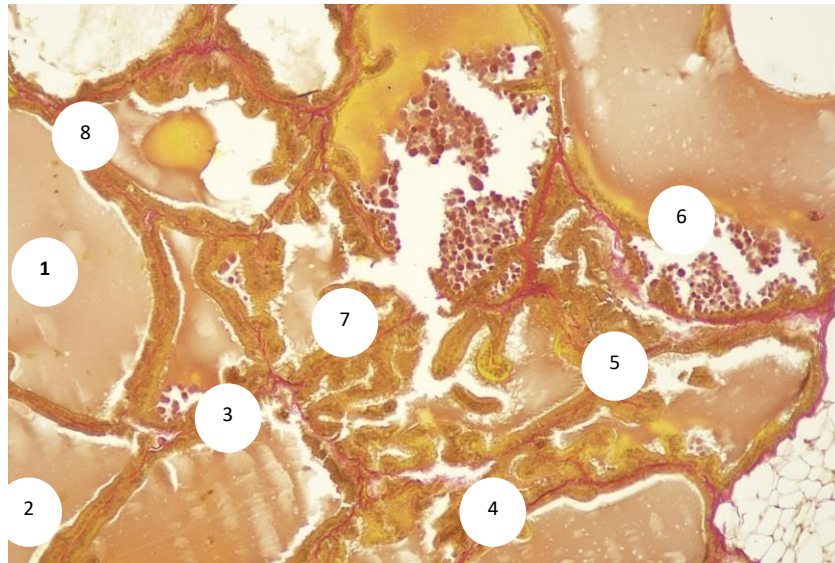
A rat's prostate at 18 months of age (Figure 2). Hematoxylin and eosin staining. 1-ovoid acini with intraluminal secretion; 2-acinus of irregular form; 3-dilated stromal septa; 4-plentiful stromal arteries; 5-diffuse acini in the stroma; 6-accumulations of lymphocytes



Rat prostate at 18 months of age (Figure 3). Hematoxylin and eosin staining. Epithelial proliferation in the prostate urethra, glandular ducts, acini, intraorgan vessels, connective tissue growth sites, cystic atrophy in hyperplastic adenomatous nodes, and plethoric intraorgan vessels. In that case, please accept 10 copies of Volume 25.

averages 32.5% 0.8%, with a range of 25-40%; no secretions are present in any of the acini's lumens. The acini lumens did not include any desquamated epithelial cells.

The experimental group's 18-month-old rats exhibit severe lymphocyte infiltration, tissue damage, and nodular development. Countless lymphocytes are layered throughout the interacinar stroma.



An 18-month-old rat's prostate (Fig. 4). Van Gieson's hues are used. Stagnant end sections of the secretory apparatus, a low-prismatic epithelium, a fibrous-muscular stroma, bundles of collagen fibers surrounding the secretory sections, a small-loop network of collagen fibers in the stroma, nodules within the acini, epithelial tears in the acinar lining, a large calculus within the secretory apparatus, and so on. OK. 10 x vol. 20.

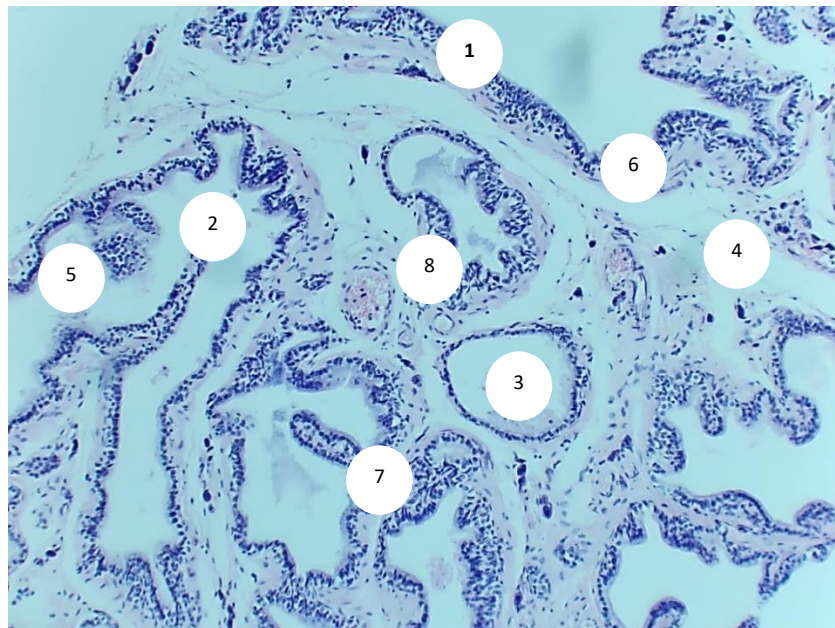


Figure. 5. The prostate of an experimental group rat aged 18 months. Hematoxylin and eosin staining. One gland capsule, two acini of various shapes and sizes, three acini lined with squamous epithelium, four dilated stromal septa with exposed areas and tissue destruction, no organ tissue structure, five diffuse accumulations of lymphocytes in the intraluminal space, six accumulations of lymphocytes in the subcapsular zone, seven accumulations of lymphocytes in the subepithelial and epithelial-stromal outgrowths, eight a profusion of OK. 10 x vol. 20.

visualized. Diffuse lymphocyte accumulations inside the lumen, in the capsular zone, the subepithelial layer, and the epithelial-stromal outgrowths are typical features of most preparations. Diffuse accumulations of lymphocytes penetrating the walls of the vessels may be

seen in a few locations near the intralobular stroma's full-blooded vessels. Lymphoid nodules of various sizes and forms (Fig. 5.7) are identified in certain specimens. Lymphocytes in the stroma (inside the field of vision) are so numerous that counting them would be impossible.

Journal of Coastal Life Medicine

Subcapsular zones and core portions of the gland show substantial connective tissue growth (the partitions are expanded in 7-8 fields of view out of 10). Bare spots, when the underlying organ tissue structure is not apparent, may be discovered in the subcapsular zone.

Between 96.6 and 231.0 μm is the average thickness of the stromal septa that separates the acini in the subcapsular zone. The stromal layers in the central prostate are between 63 and 84 microns thick.

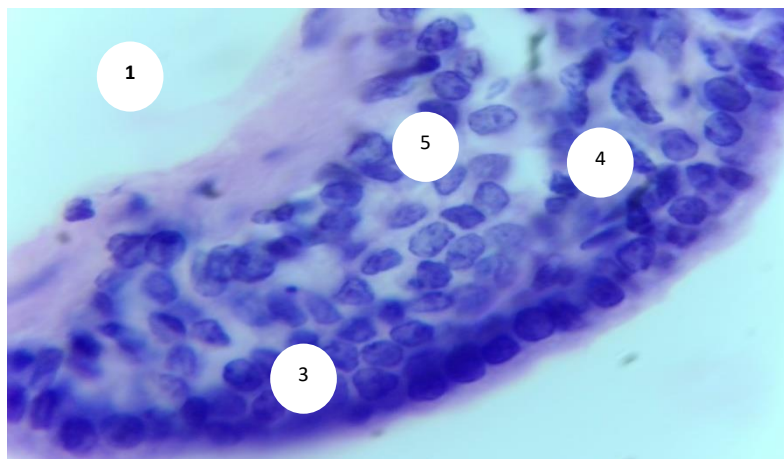


Figure .6: The prostate of an experimental group rat at 18 months of age. Hematoxylin and eosin staining. The interglandular stroma, the acinus lumen, the epithelial stratification center (with its multi-row and polymorphic cells), big, multinucleated, and mitotic cells. Ten copies of Volume 40 are fine.

It is in the interglandular stroma that the vast network of veins, arteries, and capillaries are mapped out. Combined regions of stromal hemorrhages and phenomena of stasis of generated components in the arteries are shown in Fig. 8. Within this field of view, the number of stromal vessels varies between 14 and 25, with an average of 18.80.6. Venule inner diameters are on average 42.00.9 μm but may be anything from 29.4 to 46.2 μm . Their average wall

thickness is 5.42 0.21 microns (ranging from 4.2 to 8.4 microns). Capillary diameter ranges from 16.8 to 25.2 μm , with an average of 20.12 0.42 μm . Their average wall thickness is 4.540.21 microns, with a range of 4.2-8.4 microns. Arteriole inner diameters are 16.8-21.0 μm wide, on average 19.450.21 μm . Their average wall thickness is 5.420.21 μm , with a range of 4.2-8.4 μm .

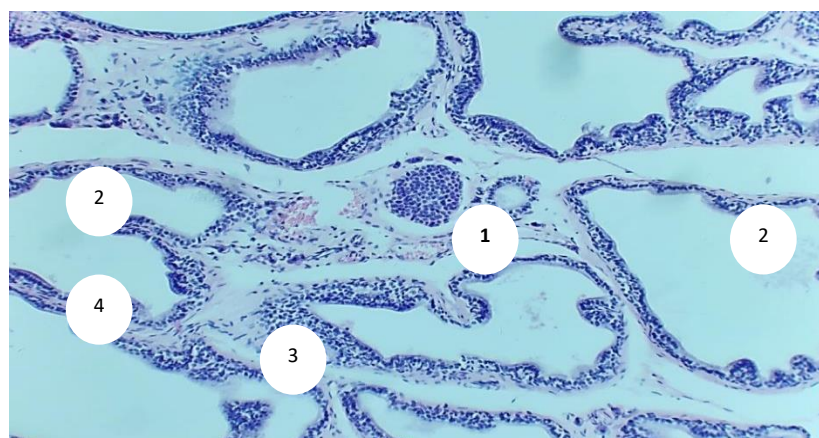


Figure 7 shows the prostate of an experimental group rat at 18 months of age. Hematoxylin and eosin staining. Irregular lymphoid nodule in the interglandular stroma; II. stromal sections devoid of tissue structure; III. stromal hemorrhages in regions; and IV. widespread lymphocyte accumulations in the subepithelial layer and epithelial-stromal protrusions. In that case, ten copies of volume 20 is OK.

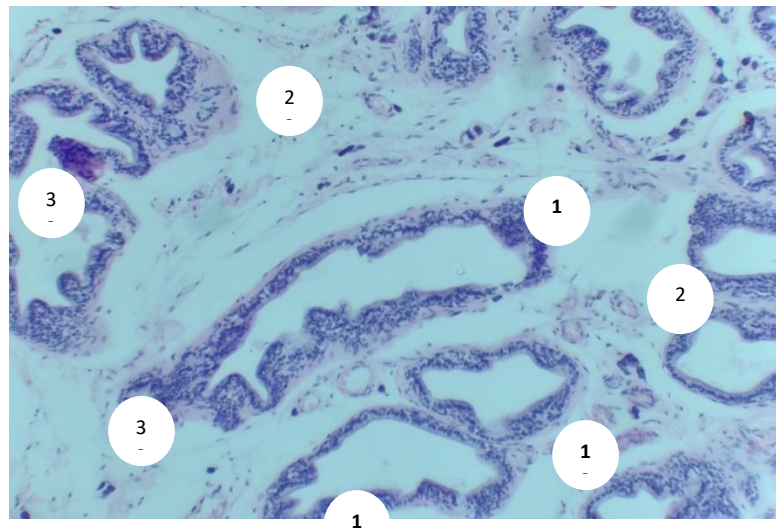


Figure .8: The prostate of an experimental group rat at 18 months of age. Hematoxylin and eosin staining. Diffuse accumulations of lymphocytes in the subepithelial layer; 1. a high density of intraorganic vessels in the interglandular stroma, indicative of stasis and plethora; 2. dilated stromal septa with bare patches; 3. In that case, please accept 10 copies of Volume 25. According to morphometric analysis of the parenchymal-stromal ratio, the average relative area of its parenchyma is 34.1% 1.4%. Stromal tissue makes up anywhere from 54% to 80% of the total tissue, with a mean of 65.11%.

Collagen fibers abnormally proliferate across the fibromuscular stroma in the experiment. Collagen fibers are generated in large numbers and eventually fill the stromal interepithelial spaces. They are located in close proximity to the gland's acini and ducts, where they tightly braid the stromal layer's smooth myocytes. The interacinar stroma sometimes develops a coarse network of collagen fibers. The average thickness of collagen fiber bundles is 7.690.21 m, however this value ranges from 4.2 to 8.4 m.

5. Conclusions

Proliferative changes in the epithelium of the secretory sections, excretory ducts, and prostatic urethra are seen in animals that are 1.5 years old; nodules are found within the acini; congestive, vascular changes are seen; a moderate degree of lymphocytic infiltration without tissue destruction and lymphoid nodular formation is also seen. The glandular parenchyma volume fraction decreases, the number and diameter of vessels increase, and the thickness of their walls decrease in chronically alcoholic animals, as well as a pronounced degree of lymphocytic infiltration, tissue destruction, and lymphoid nodular formation. The experiment results in the formation and growth of papillary structures due to involutive changes (a flattening of the acinar epithelium, a reduction in the size of the acinus, and a decrease in

secretory activity).

A strong pathological proliferation of connective tissue, expansion of stromal septa, primarily in the subcapsular zone, and thickening of bundles of collagen fibers result from chronic alcohol exposure; these changes can be interpreted as the body's attempt to isolate the site of damage from the rest of the tissues and the blood supply as a whole.

Lis To Fliteratures:

- [1] Medical Morphometry / G. G. Avtandilov. - M: Medicine, 1990. - 384 pages. 1.
- [2] Second: E.N. Gorbunova and Davydova Risk factors for prostatic intraepithelial neoplasia and prostate cancer: a review of the literature D.A. Krupin V.N. Clinical Medicine. - 2011. - No. 1. - P. 79-83
- [3] Narcology and national leadership. Ivanets N.N., I.P. Anokhina, and M.A. Vinnikova. 2016; 944 pages: M.: GEOTAR - Media.
- [4] 4. KamolovKh.Yo. Morphological features of the lung in chronic alcoholism // Journal "New Day in Medicine". - 2021. - No. 2 (34). - S. 235-237.
- [5] A.A. Muzhikyan, Ya.A. Gushchin, E.V. Belyaeva, M.N. Makarova, and V.G. Laboratory rat autopsy and organ retrieval technique // Message 1. Animals

Journal of Coastal Life Medicine

in laboratories for medical and scientific study:
2018. 2. DOI: 10.29296/10.29296/2618723X-2018-02-08.

- [6] Alcoholism, by Moiseev V.S. Toxic effects on vital organs, updated with new information for the second edition 2014, 480 M.: GEOTAR - Media.
- [7] Morphological alterations in organs in different kinds of alcoholic illness // Questions of Narcology. - 2012. - No. 3. - P. 34-40. 7. Pavlov A. L., Pavlova A. Z., Bogomolov D. V., Larev Z. V., Trofimova I. N.
- [8] Guidelines for the use of animals in toxicological research. 8. Sidorov, P.I. Arkhangelsk: P.I. Sidorova, 2002; 15 p.
- [9] 9 Khokhryakov A.V. Abstract of the thesis. dis.... cand. honey. Sciences. - Nizhny Novgorod, 2009. Morpho-functional features of the male reproductive system in acute and chronic alcohol intoxication. - 22p.10. Alcohol's impact on the heart. In: Gardner J.D. and Mouton A.J. 2015; 5(2):791-802 in Compr Physiol.
- [10] Reduction in excessive drinking as a treatment result in alcohol dependency. Gastfriend, D.R., Garbutt, J.C., Pettinati, H.M., Forman, R.F. Journal of Substance Abuse Treatment. Vol.33, No.1. (2017), pp.71-80.
- [11] Constrictor responses of cerebral resistance arterioles in male and female rats exposed to prenatal alcohol // 2019 Physiological Reports, 9, e15079 <https://doi.org/10.14814/phy2.15079> Cananzi, S., and Mayhan, W. Physiological Reports 9 (April 2019): e15079.
- [12] Postnatal ontogenetic changes in the body mass index and prostate morphological characteristics in male rats. Radjabov, A.B., British Medical Journal, 2022, volume 2, issue 1, pages 278-283.
- [13] Prostate microanatomy of adult rats and its response modifications in chronic drinking // American Journal of Medicine and Medical Sciences. 2023. Vol. 13. No. 7. Pages 867-871.